Distributed Collaborative Beamforming in the Presence of Angular Scattering

Slim Zaidi, *Student Member, IEEE*, and Sofiène Affes, *Senior Member, IEEE*

Abstract—In this paper, a collaborative beamformer (CB) is considered to achieve a dual-hop communication from a source to a receiver, through a wireless network comprised of K independent terminals. Whereas previous works neglect the scattering effect to assume a plane-wave single-ray propagation channel termed here as monochromatic (with reference to its angular distribution), a multi-ray channel termed as polychromatic due to the presence of scattering is considered, thereby broadening the range of applications in real-world environments. Taking into account the scattering effects, the weights of the so-called polychromatic CB (P-CB) are designed so as to minimize the received noise power while maintaining the desired power equal to unity. Unfortunately, their derivation in closed-form is analytically intractable due to the complex nature of polychromatic channels. However, when the angular spread (AS) is relatively small to moderate, it is proven that a polychromatic channel may be properly approximated by two rays and hence considered as bichromatic. Exploiting this fact, we introduce a new bichromatic CB (B-CB) whose weights can be derived in closed-form and, further, accurately approximate the P-CB's weights. Yet these weights, which turn out to be locally uncomputable at every terminal, are unsuitable for a distributed implementation. In order to circumvent this shortcoming, we exploit the asymptotic expression at large K of the B-CB whose weights could be locally computed at every terminal and, further, well-approximate their original counterparts. The performances of the so-obtained bichromatic distributed CB (B-DCB) and its advantages against the monochromatic DCB (M-DCB), which is designed without accounting for scattering, are analytically proved and further verified by simulations at practical values of K.

Index Terms—Distributed collaborative beamforming, scattering, angular distribution/spread, monochromatic/single-ray and polychromatic/multi-ray channels, bichromatic/two-ray approach, device/machine-2-device/machine (D2D/M2M) communications, wireless sensor networks (WSN).

I. INTRODUCTION

COLLABORATIVE beamforming (CB) stands out today to be a strong means to increase the transmission coverage, the link reliability, and the capacity of wireless networks [1]-[12]. Using CB, a set of K independent terminals (sensor nodes, mobile users, soldiers in battlefield, relays, etc.) play a central role in the data transmission between a pair source-receiver. These sensors, terminals, devices or machines, called all terminals here for simplicity, multiply their received signals

from the source with the complex conjugates of properly selected beamforming weights, and forward the resulting signals to the receiver. When the beamforming response in the desired direction is fixed, it has been shown that the transmit power is inversely proportional to K while the achieved signal-to-noise ratio (SNR) increases with K [6], [9], [11]. Since the number of terminals K is typically large in many practical cases, using CB in wireless networks results in both a substantial improvement in the signal reception quality and a considerable increase in the terminals' battery lifetime [11], [12].

Due to its practical potential, CB has garnered the attention of the research community. Assuming that the terminals are uniformly distributed, the CB concept was presented in [1] and the characteristics of its resultant beampattern were analyzed. Beampattern characteristics of the CB were also evaluated in [2] when the terminals are Gaussian distributed. In [3], a unified method to analyze the beampattern properties for various terminal distributions was proposed. To achieve improved beampattern properties, terminal selection algorithms aiming to narrow down the mainbeam and minimize the effect of sidelobes were, respectively, presented in [4] and [5]. In [6], the applicability of CB in wireless networks was investigated and several deployment solutions were explored in [7]. New CB techniques that improve the network energy efficiency and reduce the collaboration time were, respectively, presented in [8] and [9]. A review of the different CB techniques wherein properly selected weights achieve a given design's objective while satisfying its constraints was made in [10].

These selected weights must often comply with the restrictions dictated by the network structure. For instance, when a CB technique is used in a wireless network that lacks a master terminal (MT) with a global knowledge of all network parameters, the terminals are typically required to locally compute their weights based solely on their limited knowledge about the network. This is also the case when the MT is available to compute all weights but the overhead associated with sending them to all terminals is prohibitive. This impediment motivates further investigation in this direction. Lending themselves to a distributed implementation, a variety of so-called distributed CB (DCB) techniques, wherein the selected weights solely depend on the information commonly available at every terminal and, hence, each is able to locally compute its own weight, were proposed in [11] and [12].

In spite of their significant contributions, all the above works neglect the scattering and reflection effects to assume plane-wave or single-ray propagation channels termed here as monochromatic (with reference to their angular distribution). Although this assumption is useful for analytical purposes, it is

often not valid in practice. Indeed, in real-world environments, the very likely presence of scattering causes an angular spread (AS) of the transmit or receive signal. Several rays or "spatial chromatics" (with reference to their angular distribution) are then generated to form a multi-ray or polychromatic channel [13]-[18].The scattering effect on CB was investigated in [14] where the author analyzed, in the presence of scattering, the performance of a monochromatic DCB (M-DCB) technique whose design accounts for single-ray propagation channels. It was shown that the performance of the M-DCB technique deteriorates in areas where the AS is very small and becomes unsatisfactory when the AS substantially increases [14]. The aim of this work is to design a DCB technique which accounts for the scattering effect, thereby pushing farther the frontier of the DCB's real-world applicability range to include scattered environments with small to moderate angular spreads.

In this paper, we consider a CB technique to achieve a dual-hop communication from a source to a receiver, through a wireless network comprised of K independent terminals. In the first time slot, the source sends its signal to the network while, in the second time slot, each terminal multiplies its received signal by a properly selected beamforming weight and forwards the resulting signal to the receiver. These weights aim to minimize the received noise power while maintaining the desired power equal to unity. Due to the presence of scattering, we assume a polychromatic channel when designing the so-called polychromatic CB (P-CB) technique. Due to the complex nature of such a channel, derivation of closed-form expressions for the P-CB's weights turns out to be analytically intractable. However, when the AS is relatively small to moderate, the polychromatic channel, owing to a Taylor series expansion of its correlation matrix, can be properly approximated by two angular rays and hence considered as bichromatic. Exploiting this fact, we introduce a new bichromatic CB (B-CB) technique whose weights can be derived in closed-form and, further, accurately approximate those of the P-CB technique. Nevertheless, the distributed feature of our wireless network dictates every terminal to compute its beamforming weight based only on its limited locally-available information. Unfortunately, the B-CB's weights turn out to be locally uncomputable at every terminal, and, hence, this beamformer cannot be implemented in a distributed fashion. To circumvent this problem, we exploit the asymptotic expression at large K of the B-CB whose weights can be locally computed at every terminal and, further, well-approximate their original counterparts. The performances of the so-obtained B-DCB (i.e., distributed B-CB) technique are analyzed and compared to those of the M-DCB and B-CB techniques. We show that the proposed B-DCB technique is able to achieve its maximum achievable average SNR (ASNR) in scattered environments with small to moderate angular spreads while the achieved ASNR using the M-DCB technique, which is designed without accounting for scattering, decreases when the latter is small and becomes unsatisfactory at moderate values. We also show that using the proposed B-DCB technique instead of the M-DCB results in an ASNR gain that may reach as much as 3 dB, when K is large enough. Moreover, we prove that for K typically in the range of 10, the achieved ASNR using the B-DCB technique loses only a fraction of a dB against
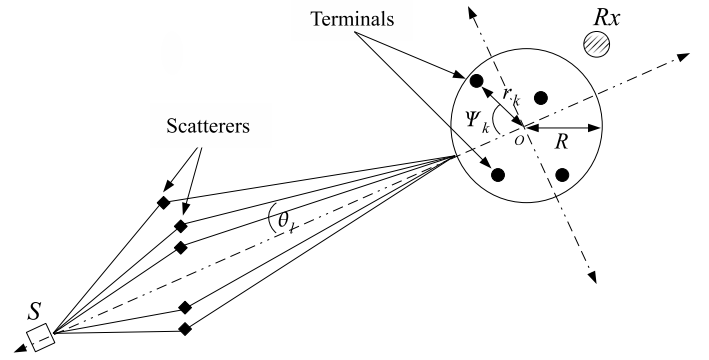

Fig. 1.   System model.

the B-CB technique, which is unsuitable for a distributed implementation.

The rest of this paper is organized as follows. The system model is described in Section II. Section III investigates the CB in the presence of scattering. The novel DCB solution that takes into account the scattering effect is proposed in Section IV. Section V analyzes the performances of the proposed technique while Section VI verifies by computer simulations the theoretical results. Concluding remarks are given in Section VII.

Notation: Uppercase and lowercase bold letters denote matrices and column vectors, respectively. $[\cdot]_{il}$ and $[\cdot]_i$ are the (i, l)-th entry of a matrix and i-th entry of a vector, respectively. $\mathbf{I}_N$ is the N-by-N identity matrix and $\mathbf{e}_n$ is a vector with one in the n-th position and zeros elsewhere. $(\cdot)^T$ and $(\cdot)^H$ denote the transpose and the Hermitian transpose, respectively. $\|\cdot\|$ is the 2-norm of a vector and $|\cdot|$ is the absolute value. $\mathrm{E}\{\cdot\}$ stands for the statistical expectation and $(\xrightarrow{ep1})$ $\xrightarrow{p1}$ denotes (element-wise) convergence with probability one. $J_1(\cdot)$ is the first-order Bessel function of the first kind and $\odot$ is the element-wise product.

II. SYSTEM MODEL

As illustrated in Fig. 1, the system of interest consists of a wireless network or subnetwork comprised of K terminals equipped each with a single isotropic antenna and uniformly and independently distributed on $D(O, R)$, the disc with center at O and radius R, a receiver Rx, and a source S both located in the same plane containing $D(O, R)$ [1]-[12], [14]. We assume that there is no direct link from the source to the receiver due to high pathloss attenuation. Moreover, let (r_k, ψ_k) denote the polar coordinates of the k-th terminal and (A_s, ϕ_s) denote those of the source. Without loss of generality, the latter is assumed to be at $\phi_s = 0$ and to be located far from the terminals, i.e., $A_s \gg R$. The following assumptions are further considered:

A1) The source is scattered by a given number of scatterers located in the same plane containing $D(O, R)$. The latters generate from the transmit signal L rays or "spatial chromatics" (with reference to their angular distribution) that form a polychromatic propagation channel [13]-[18]. The l-th ray or chromatic is characterized by its angle deviation θ_l from the source direction ϕ_s and its complex amplitude $\alpha_l = \rho_l e^{j\varphi_l}$ where the amplitudes ρ_l, $l = 1, \ldots, L$ and the

phases φ_l, $l = 1, \ldots, L$ are independent and identically distributed (i.i.d.) random variables, and each phase is uniformly distributed over $[-\pi, \pi]$. The θ_l, $l = 1, \ldots, L$ are i.i.d. zero-mean random variables with a symmetric probability density function (pdf) $p(\theta)$ and variance σ_θ^2 [14], [17], [18]. All θ_ls, φ_ls, and ρ_ls are mutually independent. All rays have equal power $1/L$ (i.e., $\mathrm{E}\{|\alpha_l|^2\} = 1/L$). Note that the standard deviation σ_θ is commonly known as the angular spread (AS) while $p(\theta)$ is called the scattering or angular distribution.

A2) The channel gain $[\mathbf{f}]_k$ from the k-th terminal to the receiver is a zero-mean unit-variance circular Gaussian random variable [9], [11].

A3) The source signal s is narrow-band[1] with unit power and noises at terminals and the receiver are zero-mean Gaussian random variables with variances σ_v^2 and σ_n^2, respectively. The source signal, noises, and the terminals' forward channel gains are mutually independent [9], [11], [12], [19].

A4) All nodes' local oscillator frequencies and phases are assumed to be synchronized by any phase/frequency adjustment techniques such as [20]-[22].

A5) The k-th terminal is aware of its own coordinates (r_k, ψ_k), its forward channel $[\mathbf{f}]_k$, the direction of the source ϕ_s, the number of terminals K, the normalized radius R/λ where λ is the wavelength, and the AS σ_θ while being oblivious to the locations and the forward channels of *all* other terminals in the network [1]-[5], [11], [12].

A1 is frequently adopted in the context of scattering environments [13]-[18] while A2-A4 are common assumptions in the array processing literature [1]-[12]. A5 which guarantees that the proposed CB technique is suitable for a distributed implementation, is commonly considered in the topic of CB [1]-[5]. Note that all parameters (position, channel, source direction, angular spread) invoked in A5 may be easily estimated using any of the existing parameters' estimation techniques, thereby inducing some estimation errors. The latters could be implicitly included in the additive Gaussian noise considered at the terminals making our scenario sufficiently realistic.

Due to A1 and the fact that $A_s \gg R$, it can be shown that the channel gain from the source to the k-th terminal can be represented as [13], [14], [18]

$$[\mathbf{g}]_k = \sum_{l=1}^{L} \alpha_l e^{-j \frac{2\pi}{\lambda} r_k \cos(\theta_l - \psi_k)}. \tag{1}$$

Obviously, in the conventional scenario where the scattering effect is neglected (i.e., $\sigma_\theta \longrightarrow 0$) to assume a monochromatic plane-wave propagation channel, we have $\theta_l = 0$ and, hence, $[\mathbf{g}]_k$ can be reduced to $[\mathbf{g}_1]_k = e^{-j(2\pi/\lambda) r_k \cos(\psi_k)}$, the well-known steering vector in the array-processing literature [1]-[5].

As can be observed from (1), the summation of L chromatics causes a variation, with a particular channel realization, of the received power at the k-th terminal. The channel is then said to experience a form of fading. When L is large, according to the Central Limit Theorem, the distribution of the channel gain $[\mathbf{g}]_k$ approaches a Gaussian. Since, according

to A1, $\mathrm{E}\{\alpha_l\} = 0$ for $l = 1, \ldots, L$, then $[\mathbf{g}]_k$ is a zero-mean Gaussian random variable and, hence, its magnitude is Rayleigh distributed. Therefore, when L is large enough (practically in the range of 10), the channel from the source to the k-th terminal is nothing but a Rayleigh channel. It can also be observed from (1) that we did not take into account any line-of-sight (LOS) component in our channel model. If this were the case, $[\mathbf{g}]_k$'s distribution would approach a non-zero mean Gaussian distribution and the channel would become Rician.

III. CB IN THE PRESENCE OF SCATTERING

A dual-hop communication is established from the source S to the receiver Rx. In the first time slot, the source sends its signal s to the wireless network. Let $\mathbf{y}$ denotes the received signal vector at the terminals given by

$$\mathbf{y} = \mathbf{g}s + \mathbf{v}, \tag{2}$$

where $\mathbf{g} \triangleq [[\mathbf{g}]_1 \ldots [\mathbf{g}]_K]^T$ and $\mathbf{v}$ is the terminals' noise vector. In the second time slot, the k-th terminal multiplies its received signal with the complex conjugate of the beamforming weight w_k and forwards the resulting signal to the receiver. It follows from (2) that the received signal at Rx is

$$
\begin{aligned}
r &= \mathbf{f}^T (\mathbf{w}^* \odot \mathbf{y}) + n = \mathbf{w}^H (\mathbf{f} \odot \mathbf{y}) + n \\
&= \mathbf{w}^H (\mathbf{f} \odot \mathbf{g}s + \mathbf{f} \odot \mathbf{v}) + n \\
&= s\mathbf{w}^H \mathbf{h} + \mathbf{w}^H (\mathbf{f} \odot \mathbf{v}) + n, \tag{3}
\end{aligned}
$$

where $\mathbf{w} \triangleq [w_1 \ldots w_K]$ is the beamforming vector, $\mathbf{h} \triangleq \mathbf{f} \odot \mathbf{g}$, $\mathbf{f} \triangleq [[\mathbf{f}]_1 \ldots [\mathbf{f}]_K]^T$, and n is the receiver noise. Let $P_{\mathbf{w},s}$ and $P_{\mathbf{w},n}$ denote the received power from the source, and the aggregate noise power due to the thermal noise at the receiver and the forwarded noises from the terminals, respectively. It holds from (3) that

$$
\begin{aligned}
P_{\mathbf{w},s} &= \mathbf{w}^H \mathrm{E}\{\mathbf{h}\mathbf{h}^H\} \mathbf{w} \tag{4} \\
P_{\mathbf{w},n} &= \sigma_v^2 \mathbf{w}^H \mathbf{\Lambda} \mathbf{w} + \sigma_n^2, \tag{5}
\end{aligned}
$$

where $\mathbf{\Lambda} \triangleq \mathrm{diag}\{|[\mathbf{f}]_1|^2 \ldots |[\mathbf{f}]_K|^2\}$ and the expectation is taken with respect to the chromatics' angles θ_ls and their complex amplitudes α_ls. Although several approaches can be adopted to properly design the beamforming weights [19], we are only concerned in this paper with minimizing the aggregate noise power while maintaining the average received power from the source equal to unity. In fact, this approach is nothing else but the well-known minimum variance distortionless response (MVDR) beamformer [23], [24] with a relaxed distortionless response constraint. The latter is imposed here to the average received power from the source (i.e., $P_{\mathbf{w},s} = 1$) instead of the instantaneous beamforming response on the source direction (i.e., $\mathbf{w}^H \mathbf{h} = 1$). Mathematically, we have to solve the following optimization problem:

$$\mathbf{w}_P = \arg \min P_{\mathbf{w},n} \qquad \text{s.t.} \qquad P_{\mathbf{w},s} = 1, \tag{6}$$

where $\mathbf{w}_P$ denotes the beamforming vector associated with the polychromatic CB[2] (P-CB). We refer to it as polychromatic since, in contrast with previous works, the channel, is assumed

---

[1]In this paper, we assume that the signal bandwith's reciprocal is large with respect to the time delays of all rays. For this reason, the time notion is ignored when denoting the source signal [13].

[2]For brevity, in this paper, we use the term CB to refer to the collaborative beamforming as well as to the collaborative beamformer.

here to be polychromatic due to the presence of scattering. The optimization problem in (6) can be rewritten as

$$\mathbf{w}_P = \arg\min \mathbf{w}^H \mathbf{\Lambda} \mathbf{w} \quad \text{s.t.} \quad \mathbf{w}^H \mathrm{E}\left\{\mathbf{h}\mathbf{h}^H\right\}\mathbf{w} = 1 \quad (7)$$

or, equivalently as

$$\mathbf{w}_P = \arg\max \frac{\mathbf{w}^H \mathrm{E}\left\{\mathbf{h}\mathbf{h}^H\right\}\mathbf{w}}{\mathbf{w}^H \mathbf{\Lambda}\mathbf{w}} \quad \text{s.t.} \quad \mathbf{w}^H \mathrm{E}\left\{\mathbf{h}\mathbf{h}^H\right\}\mathbf{w} = 1. \quad (8)$$

It can be readily shown that $\mathbf{w}_P$ is a scaled version of the principal eigenvector of the matrix $\mathbf{\Lambda}^{-1}\mathrm{E}\left\{\mathbf{h}\mathbf{h}^H\right\}$ so as to satisfy the constraint in (8) [19]. To the best of our knowledge, this eigenvector cannot be directly derived using the actual form of the matrix $\mathrm{E}\left\{\mathbf{h}\mathbf{h}^H\right\}$, thereby making impossible the derivation of $\mathbf{w}_P$ in closed-form expression. Actually, $\mathbf{w}_P$ may be numerically evaluated, but this task is computationally demanding, especially when high precision is required. There is yet another problem in that it follows from (8) that this numerical evaluation must be performed by a master terminal (MT) with a global knowledge of all network parameters and, unfortunately, according to A5, the considered network lacks such a terminal. This motivates us to derive a closed-form approximation of $\mathbf{w}_P$. To this end, a useful approximation of the matrix $\mathrm{E}\left\{\mathbf{h}\mathbf{h}^H\right\}$ may be developed which requires, however, a more in-depth analytical study beforehand. Based on assumption A1, one can deduce the following property:

$$\mathrm{E}\left\{\alpha_l^* \alpha_m\right\} = \begin{cases} 0 & l \neq m \\ \frac{1}{L} & l = m \end{cases}. \quad (9)$$

It follows from (9) that $\mathrm{E}\left\{\mathbf{h}\mathbf{h}^H\right\}$ is given by

$$\begin{aligned} \mathrm{E}\left\{\mathbf{h}\mathbf{h}^H\right\} &= \mathrm{E}\left\{\sum_{l=1}^{L}\alpha_l \mathbf{a}(\theta_l)\sum_{m=1}^{L}\alpha_m^* \mathbf{a}^H(\theta_m)\right\} \\ &= \sum_{l=1}^{L}\mathrm{E}\left\{\alpha_l \alpha_l^*\right\}\mathrm{E}\left\{\mathbf{a}(\theta_l)\mathbf{a}(\theta_l)^H\right\} \\ &= \int_{\Theta} p(\theta)\mathbf{a}(\theta)\mathbf{a}^H(\theta)d\theta, \quad (10) \end{aligned}$$

where $\mathbf{a}(\theta) \triangleq \left[[\mathbf{a}(\theta)]_1 \ldots [\mathbf{a}(\theta)]_K\right]^T$ with $[\mathbf{a}(\theta)]_k = [\mathbf{f}]_k e^{-j(2\pi/\lambda)r_k \cos(\theta - \psi_k)}$ and Θ is the span of the pdf $p(\theta)$ over which the integral is calculated[3] Nevertheless, if the AS σ_θ is relatively small[4], small angular deviations of θ_ls occur and, hence, the relationship between $\mathbf{a}(\theta)$ and θ can be accurately described by the first three non-zero terms of the Taylor series of $\mathbf{a}(\theta)$ at 0. Therefore, the following approximation holds

$$\mathbf{a}(\theta) \simeq \mathbf{a} + \mathbf{a}'\theta + \mathbf{a}''\frac{\theta^2}{2}, \quad (11)$$

where $\mathbf{a} = \mathbf{a}(0)$, and $\mathbf{a}'$ and $\mathbf{a}''$ are, respectively, the first and the second derivatives of $\mathbf{a}(\theta)$ at 0. Finally, using (11) in (10)

[3]In the Gaussian and Uniform distribution cases, $\Theta = [-\inf, +\inf]$ and $\Theta = [-\sqrt{3}\sigma_\theta, +\sqrt{3}\sigma_\theta]$, respectively.

[4]This condition is assumed for the sole sake of mathematical rigor, without imposing any limitation on AS values in absolute terms. Simulations in Section VI suggest that practical AS values as high as 20 degrees still keep the following developments valid.

and performing some mathematical manipulations yields

$$\begin{aligned} \mathrm{E}\left\{\mathbf{h}\mathbf{h}^H\right\} &\simeq \mathbf{a}\mathbf{a}^H + \frac{1}{2}\int_{\Theta} p(\theta)\left(\mathbf{a}\mathbf{a}''^H + \mathbf{a}''\mathbf{a}^H + 2\mathbf{a}'\mathbf{a}'^H\right)\theta^2 d\theta \\ &\simeq \mathbf{a}\mathbf{a}^H + \left(\mathbf{a}\mathbf{a}''^H + \mathbf{a}''\mathbf{a}^H + 2\mathbf{a}'\mathbf{a}'^H\right)\frac{\sigma_\theta^2}{2} \\ &\simeq \frac{1}{2}\left(\left(\mathbf{a} + \mathbf{a}'\sigma_\theta + \mathbf{a}''\frac{\sigma_\theta^2}{2}\right)\left(\mathbf{a} + \mathbf{a}'\sigma_\theta + \mathbf{a}''\frac{\sigma_\theta^2}{2}\right)^H + \right. \\ &\quad \left. \left(\mathbf{a} - \mathbf{a}'\sigma_\theta + \mathbf{a}''\frac{\sigma_\theta^2}{2}\right)\left(\mathbf{a} - \mathbf{a}'\sigma_\theta + \mathbf{a}''\frac{\sigma_\theta^2}{2}\right)^H\right) \\ &\simeq \frac{1}{2}\left(\mathbf{a}(\sigma_\theta)\mathbf{a}(\sigma_\theta)^H + \mathbf{a}(-\sigma_\theta)\mathbf{a}(-\sigma_\theta)^H\right). \quad (12) \end{aligned}$$

It is noteworthy that the approximation in (12) is independent of the scattering distribution $p(\theta)$. Rather, it explicitly depends on the AS σ_θ. More importantly, it can be easily proven that the result in (12) also holds in the case of bichromatic channels (i.e., $L = 2$) with rays located at angles σ_θ and $-\sigma_\theta$ where the channel gain from the source to the k-th terminal is $[\mathbf{g}_2]_k = \alpha_1 e^{-j(2\pi/\lambda)r_k \cos(\sigma_\theta - \psi_k)} + \alpha_2 e^{-j(2\pi/\lambda)r_k \cos(\sigma_\theta + \psi_k)}$. Consequently, when the AS is typically small to moderate, $\mathbf{g}$ could be substituted with $\mathbf{g}_2$ and, hence, polychromatic channels could be considered as bichromatic. This bichromatic approach is notable since it can be exploited in AS and direction of arrival estimation in scattering environments such as in [13], [17] and [18]. Furthermore, it turns out to be crucial for our new design of a CB technique that accounts for scattering. Indeed, according to the approximation in (12), when σ_θ is relatively small, we have $\mathbf{w}_P \simeq \mathbf{w}_B$ the beamforming vector associated with the bichromatic CB (B-CB) technique that satisfies

$$\mathbf{w}_B = \arg\max \frac{\mathbf{w}^H \mathbf{\Xi}\mathbf{w}}{\mathbf{w}^H \mathbf{\Lambda}\mathbf{w}} \quad \text{s.t} \quad \mathbf{w}^H \mathbf{\Xi}\mathbf{w} = 2, \quad (13)$$

where $\mathbf{\Xi} = \left(\mathbf{a}(\sigma_\theta)\mathbf{a}(\sigma_\theta)^H + \mathbf{a}(-\sigma_\theta)\mathbf{a}(-\sigma_\theta)^H\right)$. It can be shown that the optimal solution of (13) is given by [19]

$$\mathbf{w}_B = \frac{\mu}{K}\rho_{\max}\left(\mathbf{\Lambda}^{-1}\mathbf{\Xi}\right), \quad (14)$$

where $\rho_{\max}\left(\mathbf{\Lambda}^{-1}\mathbf{\Xi}\right)$ is the principal eigenvector of the matrix $\mathbf{\Lambda}^{-1}\mathbf{\Xi}$ and μ is a factor chosen such that the constraint in (13) is satisfied. Now, we have to derive the expression of the eigenvector $\rho_{\max}\left(\mathbf{\Lambda}^{-1}\mathbf{\Xi}\right)$. Since $\mathbf{\Lambda}^{-1}$ is a full-rank matrix, the rank of $\mathbf{\Lambda}^{-1}\mathbf{\Xi}$ is the same as the rank of $\mathbf{\Xi}$ that is inferior or equal to two, which means that $\mathbf{\Lambda}^{-1}\mathbf{\Xi}$ has at most two eigenvectors. In addition, it can be proven that

$$\begin{aligned} \mathbf{\Lambda}^{-1}\mathbf{\Xi}\mathbf{\Lambda}^{-1}(\mathbf{a}(\sigma_\theta)+\mathbf{a}(-\sigma_\theta)) &= \mathbf{\Lambda}^{-1}\mathbf{a}(\sigma_\theta)\,K\left(1+Z\left(\sigma_\theta\right)\right) + \\ &\quad \mathbf{\Lambda}^{-1}\mathbf{a}(-\sigma_\theta)\,K\left(1+Z\left(\sigma_\theta\right)^H\right), \end{aligned} \quad (15)$$

and

$$\begin{aligned} \mathbf{\Lambda}^{-1}\mathbf{\Xi}\mathbf{\Lambda}^{-1}(\mathbf{a}(\sigma_\theta)-\mathbf{a}(-\sigma_\theta)) &= \mathbf{\Lambda}^{-1}\mathbf{a}(\sigma_\theta)\,K\left(1-Z\left(\sigma_\theta\right)\right) - \\ &\quad \mathbf{\Lambda}^{-1}\mathbf{a}(-\sigma_\theta)\,K\left(1-Z\left(\sigma_\theta\right)^H\right), \end{aligned} \quad (16)$$

where $Z\left(\sigma_\theta\right) = \left(\mathbf{a}(\sigma_\theta)^H \mathbf{\Lambda}^{-1}\mathbf{a}(-\sigma_\theta)\right)/K$. It can be shown from the definition of $\mathbf{a}(\theta)$ that for small σ_θ

we have $|\text{Im}\{Z(\sigma_\theta)\}| \leq \sin(4\pi R\sigma_\theta/\lambda)$ and, further, $\text{Re}\{Z(\sigma_\theta)\} \geq 0$. If σ_θ is small enough[4], the imaginary part of $Z(\sigma_\theta)$ approaches 0 and, hence, the latter could be considered as positive real. Therefore, from (15) and (16), $\mathbf{\Lambda}^{-1}(\mathbf{a}(\sigma_\theta) + \mathbf{a}(-\sigma_\theta))$ and $\mathbf{\Lambda}^{-1}(\mathbf{a}(\sigma_\theta) - \mathbf{a}(-\sigma_\theta))$ are both eigenvectors of $\mathbf{\Lambda}^{-1}\mathbf{\Xi}$ and, additionally, $\rho_{\max}(\mathbf{\Lambda}^{-1}\mathbf{\Xi}) \simeq \mathbf{\Lambda}^{-1}(\mathbf{a}(\sigma_\theta) + \mathbf{a}(-\sigma_\theta))$, when σ_θ is relatively small. Consequently, $\mathbf{w}_\mathrm{B}$ can be expressed as

$$\mathbf{w}_\mathrm{B} = \frac{\mu}{K}\mathbf{\Lambda}^{-1}(\mathbf{a}(\sigma_\theta) + \mathbf{a}(-\sigma_\theta)), \tag{17}$$

where

$$\begin{aligned}\mu &\simeq \frac{\sqrt{2K}}{\left\|\mathbf{\Lambda}^{-\frac{1}{2}}(\mathbf{a}(\sigma_\theta) + \mathbf{a}(-\sigma_\theta))\right\|(1 + \text{Re}\{Z(\sigma_\theta)\})^{\frac{1}{2}}} \\ &\simeq (1 + \text{Re}\{Z(\sigma_\theta)\})^{-1}. \end{aligned} \tag{18}$$

As it can be observed from (17), $\mathbf{w}_\mathrm{B}$ is independent of the scattering distribution $p(\theta)$. Rather, it explicitly depends on σ_θ that can be estimated using an AS estimator such as in [17] or [18].

Nevertheless, since the terminals are independent entities and there is no MT with global knowledge of all network parameters, the B-CB technique is implementable only if the k-th terminal can locally compute its corresponding beamforming weight $[\mathbf{w}_\mathrm{B}]_k$ that depends on μ and the k-th entry of $\mathbf{\Lambda}^{-1}(\mathbf{a}(\sigma_\theta) + \mathbf{a}(-\sigma_\theta))/K$. According to A5, the latter depends solely on the information locally available at the k-th terminal while μ is function of all terminals' locations and forward channels and, hence, cannot be computed at every terminal. Therefore, although the B-CB is an optimal solution of (6) that takes into account the scattering effect for relatively small σ_θ, it turns out to be unsuitable for a distributed implementation in our considered network. In Section IV, a bichromatic distributed CB (B-DCB) is proposed, that not only can be implemented in a distributed fashion, but also well-approximates its B-CB counterpart.

IV. PROPOSED B-DCB TECHNIQUE

In order to circumvent the aforementioned problem, we resort to substituting μ with a quantity that can be computed at every individual terminal and, in addition, well-approximates its original counterpart. It has been shown in [6], [9] and [11] that, when the received power is fixed as in the design of the B-CB technique, the transmit power from each terminal is inversely proportional to K while the SNR linearly increases with K. This suggests the use of a large number of terminals as a means to considerably increase the terminals' battery lifetime and substantially improve the signal reception quality. Thus, when K is large enough, μ could be substituted with $\mu_\mathrm{D} = \lim_{K\to\infty}\mu$ in (17). Although μ_D seems to be a good approximation of the constraint factor μ, it must also solely depend on the information commonly available at all the terminals. This will be proved in the following lines.

It is direct to show from (18) that

$$\mu_\mathrm{D} = \left(1 + \text{Re}\left\{\lim_{K\to\infty} Z(\sigma_\theta)\right\}\right)^{-1}. \tag{19}$$

From the definition of $\mathbf{a}(\phi)$, we have

$$Z(\sigma_\theta) = \frac{\sum_{k=1}^{K} e^{j\frac{2\pi}{\lambda}r_k(\cos(\psi_k + \sigma_\theta) - \cos(\psi_k - \sigma_\theta))}}{K}. \tag{20}$$

Using the strong law of large numbers and the fact that r_k, ψ_k and $[\mathbf{f}]_k$ are all mutually statistically independent, we obtain [25], [26]

$$\begin{aligned}\lim_{K\to\infty} Z(\sigma_\theta) &\xrightarrow{p1} \mathrm{E}\left\{e^{j\frac{2\pi}{\lambda}r_k(\cos(\psi_k + \sigma_\theta) - \cos(\psi_k - \sigma_\theta))}\right\} \\ &= 2\frac{J_1(\gamma(2\sigma_\theta))}{\gamma(2\sigma_\theta)} \end{aligned} \tag{21}$$

where the equality in the second line is due to the fact that the terminals are uniformly distributed on $D(O, R)$ [1] and $\gamma(\phi) \triangleq (4\pi R/\lambda)\sin(\phi/2)$. Therefore, it follows from (19)-(21) that

$$\mu_\mathrm{D} \xrightarrow{p1} \left(1 + 2\frac{J_1(\gamma(2\sigma_\theta))}{\gamma(2\sigma_\theta)}\right)^{-1}, \tag{22}$$

when the number of terminals K is large enough. As can be observed from (22), μ_D does not depend on the locations and the forward channels of any terminal and, therefore, it is locally computable at all terminals. Substituting μ with μ_D in (17), we introduce a new B-DCB whose beamforming vector

$$\mathbf{w}_\mathrm{BD} = \frac{\mu_\mathrm{D}}{K}\mathbf{\Lambda}^{-1}(\mathbf{a}(\sigma_\theta) + \mathbf{a}(-\sigma_\theta)) \tag{23}$$

not only can be implemented in a distributed fashion, but also well-approximates its counterpart $\mathbf{w}_\mathrm{B}$, when K is large enough[5]. Moreover, it is valid for any given scattering distribution $p(\theta)$. It is worth mentioning that in the conventional scenario, where the scattering phenomenon is neglected (i.e., $\sigma_\theta \to 0$) to assume monochromatic plane-wave propagation channels, (23) reduces to

$$\mathbf{w}_\mathrm{M} = \frac{1}{K}\mathbf{\Lambda}^{-1}\mathbf{a}, \tag{24}$$

the beamforming vector associated with the monochromatic DCB (M-DCB) also known as conventional DCB [1]-[10], [14]. Note that the main shortcoming of $\mathbf{w}_\mathrm{M}$ is its obliviousness to the presence of scattering that can cause a substantial system performance degradation, as will be unambiguously illustrated later both by analysis and simulations in Sections V and VI, respectively.

V. PERFORMANCE ANALYSIS OF THE PROPOSED B-DCB TECHNIQUE

In this section, we analyze the performance of the proposed B-DCB technique and compare it with those of the M-DCB and B-CB techniques. The comparison with the M-DCB technique, which is designed without taking into account the scattering effect, highlights the performance gain if this phenomenon is considered in the design of DCB techniques. In turn, the comparison with the B-CB technique, which cannot be implemented in a distributed fashion, emphasizes the cost of using practical values of K in the design of the proposed B-DCB technique.

---

[5]We will actually see in Section VI that K in the range of 10 readily offers an acceptable approximation.

A. CB performance metrics and beampatterns

One way to prove the efficiency of the proposed B-DCB technique is undoubtedly comparing its achieved SNR with the SNR performed when either the M-DCB or B-CB technique is implemented in the network. Let $\xi_\mathbf{w}$ denote the achieved SNR using the beamforming vector $\mathbf{w}$. It follows from (4) and (5) that $\xi_\mathbf{w}$ can be expressed as

$$\xi_\mathbf{w} = \frac{P_\mathbf{w}(\phi_s)}{P_{\mathbf{w},n}}. \tag{25}$$

In (25), commonly known as the beampattern, $P_\mathbf{w}(\phi_\star) = p_\star \left| \mathbf{w}^H \sum_{l=1}^L \alpha_l \mathbf{a}(\phi_\star + \theta_l) \right|^2$ is the received power from a transmitter at direction $\phi_\star$ with power $p_\star$. Note that $\xi_\mathbf{w}$ is an excessively complex function of the random variables r_k, ψ_k and $[\mathbf{f}]_k$ for $k = 1, \ldots, K$ and α_l and θ_l for $l = 1, \ldots, L$ and, hence, a random quantity of its own. Therefore, it is practically more appealing to investigate the behavior and the properties of the achieved average-signal-to-average-noise ratio (ASANR) $\tilde{\xi}_\mathbf{w}$ given by [11], [27], [28]

$$\tilde{\xi}_\mathbf{w} = \frac{\tilde{P}_\mathbf{w}(\phi_s)}{\tilde{P}_{\mathbf{w},n}}, \tag{26}$$

where $\tilde{P}_\mathbf{w}(\phi_\star) = \mathrm{E}\{P_\mathbf{w}(\phi_\star)\}$ is called the average beampattern and $\tilde{P}_{\mathbf{w},n} = \mathrm{E}\{P_{\mathbf{w},n}\}$ is the average noise power where the expectations are taken with respect to r_k, ψ_k and $[\mathbf{f}]_k$ for $k = 1, \ldots, K$ and α_l and θ_l for $l = 1, \ldots, L$. Note that it is also interesting to study the behavior of a more practical performance measure, the average SNR (ASNR) $\bar{\xi}_\mathbf{w} = \mathrm{E}\{P_\mathbf{w}(\phi_s)/P_{\mathbf{w},n}\}$ where the expectation is taken with respect to the random variables r_k, ψ_k and $[\mathbf{f}]_k$ for $k = 1, \ldots, K$ and α_l and θ_l for $l = 1, \ldots, L$. Since $P_\mathbf{w}(\phi_s)$ and $P_{\mathbf{w},n}$ are very complicated functions of the latter random variables, deriving a closed-form expression for $\bar{\xi}_\mathbf{w}$ appears, however, to be extremely difficult if not impossible. This also suggests that it is more practical to analyze the behavior of the achieved ASANR. Yet in what follows, we will show that the achieved ASANR and ASNR using $\mathbf{w} \in \{\mathbf{w}_{\mathrm{BD}}, \mathbf{w}_{\mathrm{B}}, \mathbf{w}_{\mathrm{M}}\}$ have the same asymptotic behaviors when K grows large[6].

Let us start by deriving the expression of the achieved ASANR $\tilde{\xi}_{\mathbf{w}_{\mathrm{BD}}}$ when the proposed B-DCB technique is used in the network. To this end, we first introduce the following theorem that derives both $\tilde{P}_{\mathbf{w}_{\mathrm{BD}},n}$ and $\tilde{P}_{\mathbf{w}_{\mathrm{BD}}}(\phi_\star)$.

Theorem 1: We have

$$\tilde{P}_{\mathbf{w}_{\mathrm{BD}},n} = \frac{2\sigma_v^2}{K} \left(1 + 2\frac{J_1(\gamma(2\sigma_\theta))}{\gamma(2\sigma_\theta)}\right)^{-1} + \sigma_n^2 \tag{27}$$

and

$$\tilde{P}_{\mathbf{w}_{\mathrm{BD}}}(\phi_\star) = \frac{2p_\star}{K\left(1 + 2\frac{J_1(\gamma(2\sigma_\theta))}{\gamma(2\sigma_\theta)}\right)} \left(1 + \frac{2(K-1)\Omega(\phi_\star)}{\left(1 + 2\frac{J_1(\gamma(2\sigma_\theta))}{\gamma(2\sigma_\theta)}\right)}\right), \tag{28}$$

where

$$\Omega(\phi_\star) = \int_\Theta p(\theta) \left(\frac{J_1(\gamma(\phi_\star + \theta + \sigma_\theta))}{\gamma(\phi_\star + \theta + \sigma_\theta)} + \frac{J_1(\gamma(\phi_\star + \theta - \sigma_\theta))}{\gamma(\phi_\star + \theta - \sigma_\theta)}\right)^2 d\theta, \tag{29}$$

[6]We will actually verify by simulations in Section VI that when K is in the range of 10, the ASANR and ASNR curves almost coincide.

at any arbitrary $\phi_\star$ and $p_\star$ and for any arbitrary sets of r_k, ψ_k and $[\mathbf{f}]_k$, $k = 1, \ldots, K$ and α_l and θ_l, $l = 1, \ldots, L$.

Proof: See Appendix A.

It is noteworthy that the integrals in (29) can be computed numerically with any desired accuracy by using the most popular mathematical software packages such as Matlab or Mathematica, after properly choosing the scattering distribution $p(\theta)$. In fact, several statistical distributions for θ_l have been proposed so far such as the Laplace, Gaussian or Uniform distribution [13]-[18]. Moreover, it is straightforward to show that $\Omega(\phi) \leq \Omega(\phi_s = 0)$ and, hence, $\tilde{P}_{\mathbf{w}_{\mathrm{BD}}}(\phi_\star) \leq \tilde{P}_{\mathbf{w}_{\mathrm{BD}}}(\phi_s = 0)$. The average receive beampattern has then a peak at the source direction. This proves that the proposed B-DCB promotes the signal received from the desired direction by decreasing the received signal power from the other directions. Furthermore, it can be shown that $J_1(\gamma(2\sigma_\theta))/\gamma(2\sigma_\theta) \to 1/2$ if $\sigma_\theta \to 0$ [11], [12]. It follows then from (28) that the average received power from the source $\tilde{P}_{\mathbf{w}_{\mathrm{BD}}}(0)$ reaches its maximum value 1 when $\sigma_\theta \to 0$ (i.e., there is no scattering and, hence, the channel is monochromatic). In Section VI, it will be verified by simulations that for a relatively small to moderate σ_θ, $\tilde{P}_{\mathbf{w}_{\mathrm{BD}}}(0)$ remains equal to unity when σ_θ increases. Therefore, the proposed B-DCB is robust against the scattering effect in terms of average received power from the desired direction, when σ_θ is relatively small to moderate. On the other hand, using (27) and (28), the achieved ASANR $\tilde{\xi}_{\mathbf{w}_{\mathrm{BD}}}$ is given by

$$\tilde{\xi}_{\mathbf{w}_{\mathrm{BD}}} = \frac{1 + 2(K-1)\Omega(0)\left(1 + 2\frac{J_1(\gamma(2\sigma_\theta))}{\gamma(2\sigma_\theta)}\right)^{-1}}{\sigma_v^2 + \sigma_n^2 \frac{K}{2}\left(1 + 2\frac{J_1(\gamma(2\sigma_\theta))}{\gamma(2\sigma_\theta)}\right)}. \tag{30}$$

As can be observed from (30), the proposed B-DCB achieves its maximum achievable ASANR

$$\tilde{\xi}_{\max} = \frac{1}{\frac{\sigma_v^2}{K} + \sigma_n^2}, \tag{31}$$

when $\sigma_\theta \to 0$. Simulations in Section VI will also show that, when σ_θ is relatively small to moderate, the proposed B-DCB is able to achieve $\tilde{\xi}_{\max}$. This further proves the robustness of the proposed beamformer against the scattering effect. However, when σ_θ is relatively large, one can easily show that $J_1(\gamma(2\sigma_\theta))/\gamma(2\sigma_\theta) \simeq 0$ [1], [12]. In such a case, it can then be inferred from (30) that $\tilde{\xi}_{\mathbf{w}_{\mathrm{BD}}}$ is an affine function of $\Omega(0)$ with a positive slope. Since $\Omega(0)$ decreases if σ_θ increases, the achieved ASANR $\tilde{\xi}_{\mathbf{w}_{\mathrm{BD}}}$ turns out to be a decreasing function of σ_θ when the latter is large. In the following, we will show that even though in such highly-scattered environments the ASANR achieved using the proposed B-DCB technique deteriorates, it remains much higher than that achieved using the M-DCB technique. Now, let us focus on the latter technique. When the M-DCB technique is implemented, the following theorem holds.

Theorem 2: We have

$$\tilde{P}_{\mathbf{w}_{\mathrm{M}},n} = \frac{\sigma_v^2}{K} + \sigma_n^2 \tag{32}$$

and

$$\tilde{P}_{\mathbf{w}_{\mathrm{M}}}(\phi_\star) = \frac{p_\star}{K}(1 + (K-1)\Gamma(\phi_\star)), \tag{33}$$

where

$$\Gamma(\phi_\star) = \int_\Theta p(\theta_\star) \left(2 \frac{J_1(\gamma(\phi_\star + \theta))}{\gamma(\phi_\star + \theta)} \right)^2 d\theta, \qquad (34)$$

at any arbitrary $\phi_\star$ and $p_\star$ and for any arbitrary sets of r_k, ψ_k and $[\mathbf{f}]_k$, $k = 1, \ldots, K$ and α_l and θ_l, $l = 1, \ldots, L$.

Proof: See Appendix B.

Note that the discussion involving the integral in (29) also holds for the integral in (34). Nevertheless, assuming that the scattering distribution is Uniform over $[-\Delta, \Delta]$ (i.e., $p(\theta) = 1/2\Delta$) such as in [13], an approximation of $\Gamma(\phi_s = 0)$ expressed in terms of an infinite sum is proposed in [14] for a relatively small σ_θ. Here, a much more simpler approximation is developed. Indeed, under these conditions, $\gamma(\theta) \simeq 2\pi(R/\lambda)\theta$ and, hence, after performing some mathematical manipulations, we obtain [29]

$$\Gamma(0) \simeq \frac{1}{2(\pi R)^2 \Delta} \int_{-\Delta}^{\Delta} \left(\frac{J_1\left(2\pi\frac{R}{\lambda}\theta\right)}{\theta} \right)^2 d\theta$$

$$\simeq \frac{1}{2\Delta} \int_{-\Delta}^{\Delta} {}_2F_3\left(2, \frac{3}{2}; 2, 2, 3, -4\pi^2\left(\frac{R}{\lambda}\right)^2 \theta^2\right)$$

$$\simeq \frac{1}{2} \int_0^1 \frac{{}_2F_3\left(2, \frac{3}{2}; 2, 2, 3, -12\pi^2\left(\frac{R}{\lambda}\right)^2 \sigma_\theta^2 \theta\right)}{\sqrt{\theta}} d\theta$$

$$\simeq {}_3F_4\left(\frac{1}{2}, 2, \frac{3}{2}; \frac{3}{2}, 2, 2, 3, -12\pi^2\left(\frac{R}{\lambda}\right)^2 \sigma_\theta^2\right), (35)$$

where ${}_3F_4\left(\frac{1}{2}, 2, \frac{3}{2}; \frac{3}{2}, 2, 2, 3, -12\pi^2(R/\lambda)^2 x^2\right)$ is the hypergeometric function. Since the latter decreases with x, it follows from (33) and (35) that when σ_θ is relatively small to moderate, the average received power at the desired direction $\tilde{P}_{\mathbf{w}_M}(0)$ decreases when σ_θ increases. This is in contrast with our proposed B-DCB technique whose average received power $\tilde{P}_{\mathbf{w}_{BD}}(0)$ remains constant even though σ_θ increases in such lightly- to moderately-scattered environments. Therefore, the proposed B-DCB is more robust against the scattering effect than its M-DCB vis-a-vis, which is designed without taking into account this phenomenon. In addition, from (32) and (33), the achieved ASANR using the M-DCB technique is given by

$$\tilde{\xi}_{\mathbf{w}_M} = \frac{1 + (K-1)\Gamma(0)}{\sigma_v^2 + K\sigma_n^2}. \qquad (36)$$

Using (35) in (36), we readily show that when σ_θ is relatively small to moderate, in contrast to $\tilde{\xi}_{\mathbf{w}_{BD}}$, $\tilde{\xi}_{\mathbf{w}_M}$ is a decreasing function of σ_θ. This further proves the advantage of using the proposed B-DCB instead of the M-DCB, which is designed without taking into account the scattering effect.

Concerning the achieved ASANR using the B-CB technique $\mathbf{w}_B$, it turns out that both the beampattern $P_{\mathbf{w}_B}(\phi_\star)$ and the received noise power $P_{\mathbf{w}_B,n}$ are ratios of the random variables r_k, ψ_k and $[\mathbf{f}]_k$ for $k = 1, \ldots, K$ and α_l and θ_l for $l = 1, \ldots, L$. Therefore, deriving a closed-form expression of the average beampattern $\tilde{P}_{\mathbf{w}_B}(\phi_\star)$ and the average noise power $\tilde{P}_{\mathbf{w}_B,n}$ appears to be extremely difficult if not impossible. While this fact hampers a rigorous analytical study of the achieved ASANR $\tilde{\xi}_{\mathbf{w}_B}$, some important properties of $\tilde{\xi}_{\mathbf{w}_B}$ are derived in Section V-C and V-D, in the asymptotic regime when $K \to \infty$.

B. Asymptotic ASANR performance of B-DCB vs. M-DCB

In this section, we carry out an analytical comparison between the achieved ASANR using the proposed B-DCB technique and that achieved using the M-DCB technique. Using the fact that $J_1(\gamma(2\sigma_\theta))/\gamma(2\sigma_\theta) \to 1/2$ if $\sigma_\theta \to 0$ [11], [12], it is straightforward to show from (30) and (36) that $\tilde{\xi}_{\mathbf{w}_{BD}} = \tilde{\xi}_{\mathbf{w}_M} = \tilde{\xi}_{\max}$ if $\sigma_\theta \to 0$. This is expected since $\mathbf{w}_{BD}$ boils down to $\mathbf{w}_M$ in such a case where the channel is monochromatic and, hence, the assumption made when designing $\mathbf{w}_M$ is valid. Moreover, it is direct to show from (30) and (36) that

$$\lim_{K \to \infty} \frac{\tilde{\xi}_{\mathbf{w}_M}}{\tilde{\xi}_{\mathbf{w}_{BD}}} = \frac{\Gamma(0)\left(1 + 2\frac{J_1(\gamma(2\sigma_\theta))}{\gamma(2\sigma_\theta)}\right)^2}{4\Omega(0)}. \qquad (37)$$

When the AS σ_θ is relatively small to moderate, the relationship between σ_θ and either $J_1(\gamma(\theta + \sigma_\theta))/\gamma(\theta + \sigma_\theta)$ or $J_1(\gamma(\theta - \sigma_\theta))/\gamma(\theta - \sigma_\theta)$ can be accurately described by the first two non-zero terms of the Taylor series of the latter functions at θ as follows

$$\frac{J_1(\gamma(\theta + \sigma_\theta))}{\gamma(\theta + \sigma_\theta)} = \frac{J_1(\gamma(\theta))}{\gamma(\theta)} + \sigma_\theta \left(\frac{J_1(\gamma(x))}{\gamma(x)}\right)'\Big|_{x=\theta} \quad (38)$$

$$\frac{J_1(\gamma(\theta - \sigma_\theta))}{\gamma(\theta + \sigma_\theta)} = \frac{J_1(\gamma(\theta))}{\gamma(\theta)} - \sigma_\theta \left(\frac{J_1(\gamma(x))}{\gamma(x)}\right)'\Big|_{x=\theta}, (39)$$

where $(J_1(\gamma(x))/\gamma(x))'$ is the first derivative of $J_1(\gamma(x))/\gamma(x)$. If we substitute (38) and (39) in (29) we obtain that $\Omega(0) = \Gamma(0)$ when the AS is relatively small to moderate. Therefore, using the fact that $\sin(\sigma_\theta) \simeq \sigma_\theta$ for small σ_θ, it directly follows from (37) that

$$\lim_{K \to \infty} \frac{\tilde{\xi}_{\mathbf{w}_M}}{\tilde{\xi}_{\mathbf{w}_{BD}}} \simeq \frac{1}{4}\left(1 + {}_0F_1\left(; 2; -4\pi^2\left(\frac{R}{\lambda}\right)^2 \sigma_\theta^2\right)\right)^2. \qquad (40)$$

Since the hypergeometric function ${}_0F_1\left(; 2; -4\pi^2 x^2\right)$ decreases inversely proportional to x when the latter is small, the above approximation establishes that for large K, the ASANR gain achieved using $\mathbf{w}_{BD}$ instead of $\mathbf{w}_M$ in lightly- to moderately-scattered environments increases proportionally to σ_θ and R/λ. This proves the advantage of taking into account the scattering effect in the design of the DCB techniques.

Furthermore, when σ_θ is large in highly-scattered environments, assuming that the scattering distribution $p(\theta)$ is Uniform on $[-\Delta, \Delta]$ and using the fact that $J_1(\gamma(2\sigma_\theta))/\gamma(2\sigma_\theta) \simeq 0$ for large σ_θ, we show that

$$\Omega(0) \simeq \frac{1}{\sqrt{3}\sigma_\theta} \int_0^{\sqrt{3}\sigma_\theta} \left(\frac{J_1(\gamma(\theta - \sigma_\theta))}{\gamma(\theta - \sigma_\theta)} \right)^2 d\theta$$

$$\simeq \frac{\Gamma(0)}{2} - \frac{1}{\sqrt{3}\sigma_\theta}\left(\underbrace{\int_{-\sqrt{3}\sigma_\theta}^{-\sigma_\theta} \left(\frac{J_1(\gamma(\theta))}{\gamma(\theta)} \right)^2 d\theta}_{\simeq 0} + \right.$$

$$\left. \underbrace{\int_{(\sqrt{3}-1)\sigma_\theta}^{\sqrt{3}\sigma_\theta} \left(\frac{J_1(\gamma(\theta))}{\gamma(\theta)} \right)^2 d\theta}_{\simeq 0} \right). \qquad (41)$$

Thus, using (41) in (37) yields

$$\lim_{K \to \infty} \frac{\tilde{\xi}_{\mathbf{w}_M}}{\tilde{\xi}_{\mathbf{w}_{BD}}} \simeq \frac{1}{2}. \qquad (42)$$

Therefore, when σ_θ is large in highly-scattered environments, the ASANR gain achieved using $\mathbf{w}_{\mathrm{BD}}$ instead of $\mathbf{w}_{\mathrm{M}}$ is approximatively as much as 3 dB. This further proves the advantage of using the proposed B-DCB technique instead of the M-DCB, which is designed without taking into account the scattering effect.

Recall that both the B-DCB and the M-DCB are designed assuming perfect knowledge of the terminals' parameters (forward and backward channels, source direction, angular spread, etc.) and, hence, the comparison made above does not account for any parameter estimation error. Note that, in [30] and [31], we have already analyzed the impact of these errors on the performance of both the B-DCB and M-DCB. It has been shown that in practical conditions (including feedback quantization errors and Doppler effect), the proposed B-DCB outperforms not only the M-DCB, but also the optimal CSI-based CB for almost the entire range of practical angular spread values.

C. Asymptotic ASANR performance of B-DCB vs. B-CB

Since the proposed B-DCB $\mathbf{w}_{\mathrm{BD}}$ approximates its B-CB $\mathbf{w}_{\mathrm{B}}$ counterpart, it is expected that $\tilde{\xi}_{\mathbf{w}_{\mathrm{BD}}} \leq \tilde{\xi}_{\mathbf{w}_{\mathrm{B}}}$ and, hence, an ASANR deterioration may occur due to the approach developed in Section IV. However, when the number of terminals K is large enough, the following theorem holds.

Theorem 3: Regardless of σ_θ, we have

$$\lim_{K\to\infty} \tilde{\xi}_{\mathbf{w}_{\mathrm{BD}}} = \lim_{K\to\infty} \tilde{\xi}_{\mathbf{w}_{\mathrm{B}}}, \tag{43}$$

for any arbitrary sets of r_k, ψ_k and $[\mathbf{f}]_k$, $k = 1, \ldots, K$ and α_l and θ_l, $l = 1, \ldots, L$ and for any scattering distribution $p(\theta)$.

Proof: See Appendix C.

It follows from Theorem 3 that the B-DCB and the B-CB which cannot be implemented in a distributed fashion, achieve the same ASANR for large K. Consequently, there is no ASANR degradation due to the approach used in Section IV, when the number of terminals K is large enough, actually typically in the range of 10 as will be shown by simulations.

To summarize, thus far, we showed that using the proposed B-DCB $\mathbf{w}_{\mathrm{BD}}$ instead of the M-DCB $\mathbf{w}_{\mathrm{M}}$, which is designed without taking into account the scattering effect, results in an ASANR gain that may reach as much as 3 dB for large σ_θ. We also showed that the proposed B-DCB $\mathbf{w}_{\mathrm{BD}}$ which approximates the B-CB $\mathbf{w}_{\mathrm{B}}$, unsuitable for a distributed implementation, achieves the same ASANR as $\mathbf{w}_{\mathrm{B}}$ when K is large enough. These results highlight the efficiency, in terms of achieved ASANR, of the proposed beamformer that takes into account the scattering effect and, further, could be implemented in a distributed fashion.

D. Asymptotic equivalence between ASANR and ASNR metrics

Although the ASANR is a meaningful performance measure, the ASNR remains a more revealing metric that may provide practical system information. This fact motivates us to claim the following important theorem.

Theorem 4: Using any CB version $\mathbf{w} \in \{\mathbf{w}_{\mathrm{BD}}, \mathbf{w}_{\mathrm{B}}, \mathbf{w}_{\mathrm{M}}\}$ in the network, we have

$$\lim_{K\to\infty} \tilde{\xi}_{\mathbf{w}} = \lim_{K\to\infty} \bar{\xi}_{\mathbf{w}}, \tag{44}$$

for any arbitrary sets of r_k, ψ_k and $[\mathbf{f}]_k$, $k = 1, \ldots, K$ and α_l and θ_l, $l = 1, \ldots, L$ and for any scattering distribution $p(\theta)$.

Proof: See Appendix D.

Theorem 4 establishes that the achieved ASANR $\tilde{\xi}_{\mathbf{w}}$ and ASNR $\bar{\xi}_{\mathbf{w}}$ using $\mathbf{w} \in \{\mathbf{w}_{\mathrm{BD}}, \mathbf{w}_{\mathrm{B}}, \mathbf{w}_{\mathrm{M}}\}$ have the same behaviors when K is large enough, typically in the range of 10 as will be shown by simulations. Consequently, the proposed B-DCB is also much more efficient in terms of achieved ASNR than the M-DCB, which is designed without taking into account the scattering effect, and able to perform as much as 3 dB of ASNR gain. Furthermore, the proposed beamformer and the B-CB, which cannot be implemented in a distributed fashion achieves the same ASNR, for large K. Simulations results, in the next section, further verify and validate the efficiency of the proposed B-DCB.

Note that we have only focused in this work on the receive CB configuration, but all the derivations, solutions and results provided herein easily extend to the transmit CB configuration as well (where the source and the receiver switch positions) [25], [26]. It is also noteworthy that we have been able in [32] to extend the novel B-DCB designs to the case wherein the propagation model not only accounts for scattering, but also for the presence of interfering sources.

VI. SIMULATION RESULTS

Computer simulations are provided to support the theoretical results. All the empirical average quantities are obtained by averaging over 10^6 random realizations of r_k, ψ_k, $[\mathbf{f}]_k$ for $k = 1, \ldots, K$ and α_l, θ_l for $l = 1, \ldots, L$. In all simulations, we assume that the number of rays or chromatics is $L = 6$, the noises' powers σ_n^2 and σ_v^2 are 10 dB below the source transmit power $p_s = 1$. All curves are plotted for $R/\lambda = 1$ except those in Figs. 2(b) and 2(d).

Fig. 2 plots the average beampatterns $\tilde{P}_{\mathbf{w}_{\mathrm{BD}}}(\phi_\star)$ and $\tilde{P}_{\mathbf{w}_{\mathrm{M}}}(\phi_\star)$ for $K = 20$ and different values of R/λ and σ_θ. In this figure, two scattering distributions $p(\theta)$ are assumed: Uniform and Gaussian. As can be observed from this figure, when the AS σ_θ is small, regardless of the scattering distribution, $\tilde{P}_{\mathbf{w}_{\mathrm{M}}}(0)$ decreases if σ_θ and or R/λ increases while $\tilde{P}_{\mathbf{w}_{\mathrm{BD}}}(0)$ remains equal to unity. Therefore, when the AS is relatively small to moderate, the proposed B-DCB is more robust than its M-DCB vis-a-vis against the scattering effect, in terms of average received power from the desired direction. This observation holds if the scattering distribution is Uniform or Gaussian and can be easily verified for any other distribution.

Fig. 3 displays the analytical and the empirical ASANRs of $\mathbf{w}_{\mathrm{BD}}$ and $\mathbf{w}_{\mathrm{M}}$ as well as their empirical ASNRs versus the AS σ_θ for $K = 20$. The empirical ASANR of $\mathbf{w}_{\mathrm{P}}$ is also shown in this figure. The scattering distribution is assumed to be Uniform in Fig. 3(a) and Gaussian in Fig. 3(b). From these figures, we confirm that analytical $\tilde{\xi}_{\mathbf{w}_{\mathrm{BD}}}$ and $\tilde{\xi}_{\mathbf{w}_{\mathrm{M}}}$ match perfectly their empirical counterparts. Both figures show that the P-CB is able to achieve the maximum achievable ASNR for any given σ_θ even in highly-scattered environments. This is due to the
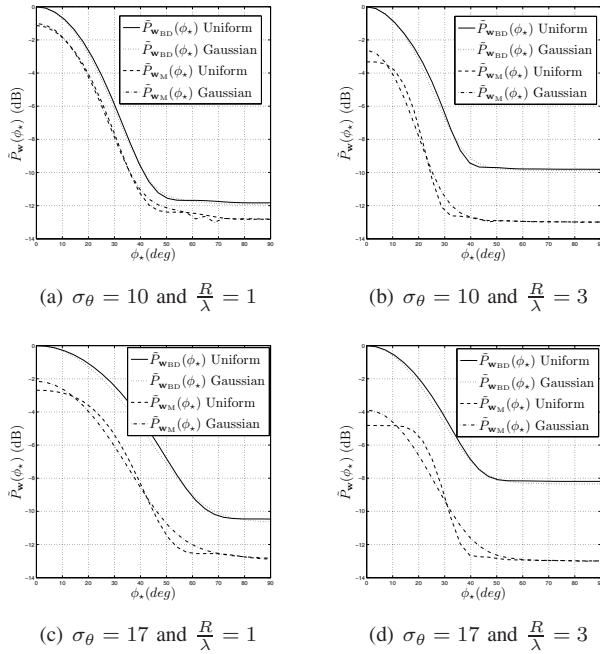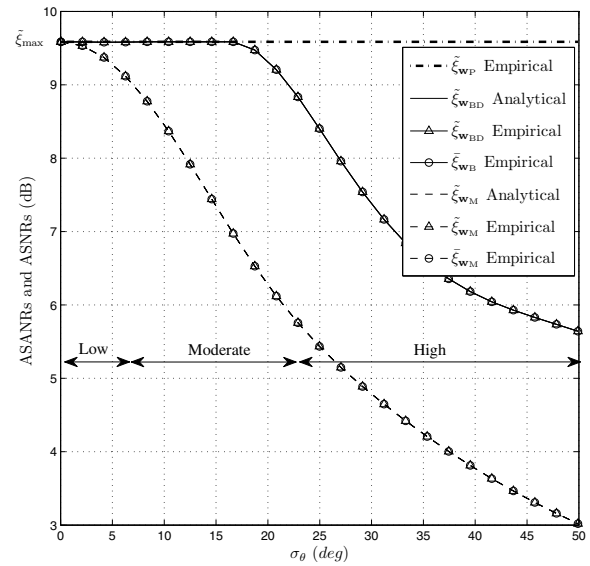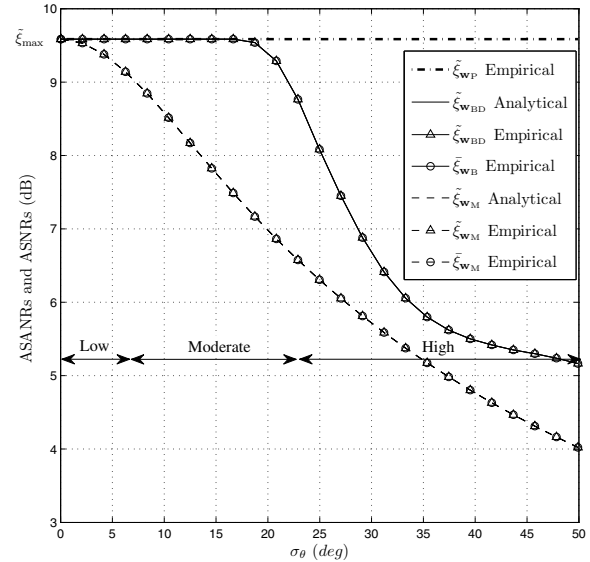
(a) $\sigma_\theta = 10$ and $\frac{R}{\lambda} = 1$ (b) $\sigma_\theta = 10$ and $\frac{R}{\lambda} = 3$

(c) $\sigma_\theta = 17$ and $\frac{R}{\lambda} = 1$ (d) $\sigma_\theta = 17$ and $\frac{R}{\lambda} = 3$

Fig. 2. The average beampatterns of $\mathbf{w}_{\mathrm{BD}}$ and $\mathbf{w}_{\mathrm{M}}$ for $\sigma_\theta = 10, 17$ (deg), $R/\lambda = 1, 3$, and $K = 20$ when the scattering distribution is Uniform and Gaussian.

optimality of the polychromatic solution. Furthermore, form these figures, we observe that the proposed B-DCB technique is able to obtain the maximum achievable ASANR $\tilde{\xi}_{\max}$ even in moderately-scattered environments where σ_θ is in the range of 20 degrees, while the ASANR performed by its M-DCB vis-a-vis decreases by 0.5 dB in lightly-scattered environments where σ_θ is around 5 degrees and becomes soon unsatisfactory in moderately- to highly-scattered environments. Furthermore, in highly-scattered environments, the proposed technique is able to achieve as much as 3 dB of ASANR gain. This corroborates the analytical result in Section V-B. Moreover, it can be observed from Figs. 3(a) and 3(b) that the curves of $\tilde{\xi}_{\mathbf{w}_{\mathrm{BD}}}$ and $\tilde{\xi}_{\mathbf{w}_{\mathrm{M}}}$ are indistinguishable from $\bar{\xi}_{\mathbf{w}_{\mathrm{BD}}}$ and $\bar{\xi}_{\mathbf{w}_{\mathrm{M}}}$, respectively, when $K = 20$. This is due to the fact that the achieved ASANRs and ASNRs have the same behaviors when K is large as claimed in Theorem 4.

Fig. 4 shows the ASANRs $\tilde{\xi}_{\mathbf{w}_{\mathrm{BD}}}$ and $\tilde{\xi}_{\mathbf{w}_{\mathrm{B}}}$ and the ASNRs $\bar{\xi}_{\mathbf{w}_{\mathrm{BD}}}$ and $\bar{\xi}_{\mathbf{w}_{\mathrm{B}}}$ versus the AS σ_θ for $K = 5, 10, 20$, when the scattering distribution is Uniform and Gaussian. It can be verified from this figure that the proposed B-DCB and the B-CB techniques always achieve the same ASANR when σ_θ is relatively small to moderate, even for small K. This is due to the fact that, regardless of the number of terminals K, $\mu_{\mathrm{D}} \simeq \mu$ for relatively small σ_θ and, hence, $\mathbf{w}_{\mathrm{BD}} \simeq \mathbf{w}_{\mathrm{B}}$. Moreover, as can be observed from Figs. 4(a) and 4(b), the curves $\tilde{\xi}_{\mathbf{w}_{\mathrm{BD}}}$ and $\bar{\xi}_{\mathbf{w}_{\mathrm{BD}}}$ as well as $\tilde{\xi}_{\mathbf{w}_{\mathrm{B}}}$ and $\bar{\xi}_{\mathbf{w}_{\mathrm{B}}}$ always coincide when σ_θ is relatively small. This is expected since $P_{\mathbf{w}_{\mathrm{B}},n} \simeq P_{\mathbf{w}_{\mathrm{BD}},n} \simeq \sigma_v^2/K + \sigma_n^2$ for relatively small σ_θ and, therefore, $\bar{\xi}_{\mathbf{w}} = \mathrm{E}\{P_{\mathbf{w}}(\phi_s)/P_{\mathbf{w},n}\} \simeq \mathrm{E}\{P_{\mathbf{w}}(\phi_s)\}/P_{\mathbf{w},n} = \tilde{\xi}_{\mathbf{w}}$ for $\mathbf{w} \in \{\mathbf{w}_{\mathrm{BD}}, \mathbf{w}_{\mathrm{B}}\}$. This further proves that the ASANR is a meaningful performance measure. Furthermore, if σ_θ is large in highly-scattered environments, the achieved ASANR using the proposed beamformer fits perfectly with that achieved using the B-CB, which is unsuitable for a distributed imple-
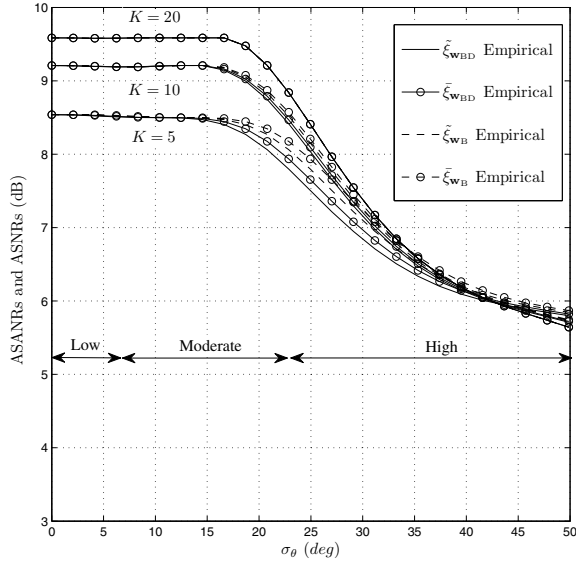

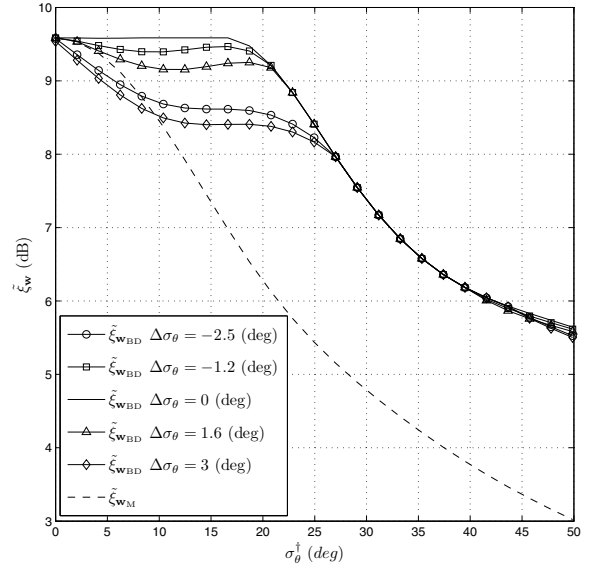(a) Uniform distribution

(b) Gaussian distribution

Fig. 3. The analytical and the empirical ASANRs achieved by $\mathbf{w}_{\mathrm{BD}}$ and $\mathbf{w}_{\mathrm{M}}$ as well as their empirical ASNRs versus σ_θ for $K = 20$ when the scattering distribution is Uniform and Gaussian (compared to the empirical ASANR achieved by $\mathbf{w}_{\mathrm{P}}$).

mentation, when K is in the range of 20 while it looses only a fraction of a dB when K is in the range of 10. It can also be observed from Figs. 4(a) and 4(b) that $\tilde{\xi}_{\mathbf{w}_{\mathrm{BD}}}$ and $\tilde{\xi}_{\mathbf{w}_{\mathrm{B}}}$ perfectly match $\bar{\xi}_{\mathbf{w}_{\mathrm{BD}}}$ and $\bar{\xi}_{\mathbf{w}_{\mathrm{B}}}$, respectively, for $K = 20$. All these observations corroborate the results in Theorems 3 and 4.

Fig. 5 plots the ASANRs $\tilde{\xi}_{\mathbf{w}_{\mathrm{M}}}$ and $\tilde{\xi}_{\mathbf{w}_{\mathrm{BD}}}$ for $K = 20$ when the estimated AS is corrupted by a deterministic estimation error $\Delta\sigma_\theta \in \{-2.5, -1.2, 0, 1.6, 3\}$. In such a case $\sigma_\theta = \sigma_\theta^\dagger + \Delta\sigma_\theta$ where $\sigma_\theta^\dagger$ is the actual AS. The scattering distribution is assumed to be Uniform in Fig. 5(a) and Gaussian in Fig. 5(b). These figures show that the proposed B-DCB technique is sensitive to AS estimation errors when the actual AS $\sigma_\theta^\dagger$ is relatively small to moderate. Nevertheless,
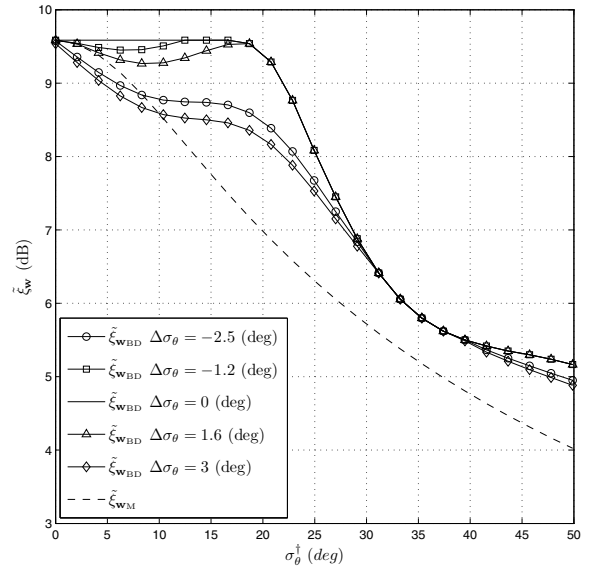
(a) Uniform distribution

(b) Gaussian distribution

Fig. 4. The empirical ASANRs and ASNRs achieved by $\mathbf{w}_{\mathrm{BD}}$ and $\mathbf{w}_{\mathrm{B}}$ versus σ_θ for $K = 5, 10, 20$ when the scattering distribution is Uniform and Gaussian.

(a) Uniform distribution

(b) Gaussian distribution

Fig. 5. The ASANRs $\tilde{\xi}_{\mathbf{w}_{\mathrm{BD}}}$ and $\tilde{\xi}_{\mathbf{w}_{\mathrm{M}}}$ versus the actual $\sigma_\theta^\dagger$ for $K = 20$, and different AS estimation errors when the scattering distribution is Uniform and Gaussian.

the ASANR degradation caused by such an error remains acceptable provided that $\Delta\sigma_\theta$ is kept reasonable. Fig. 5 shows on the other hand that, regardless of the scattering distribution, the proposed technique is quite robust to AS estimation errors when $\sigma_\theta^\dagger$ is large in highly-scattered environments. This is expected since, in such areas, $\Delta\sigma_\theta$ is negligible compared to $\sigma_\theta^\dagger$ and, hence, $\sigma_\theta \simeq \sigma_\theta^\dagger$.

VII. CONCLUSION

Whereas previous works neglected the scattering effect to assume a monochromatic channel, in this paper, a poly-chromatic channel due to the presence of scattering was assumed. We considered a P-CB technique to achieve a dual-

hop communication from a source to a receiver, through a wireless network comprised of K independent terminals. Due to the complex nature of polychromatic channels, the design of this technique both in closed-form and in distributed fashion is impossible. Using the fact that, for a relatively small to moderate AS, a polychromatic channel may be considered as bichromatic, we introduced a new B-CB technique that can be easily designed in closed-form and, further, accurately approximates the P-CB technique. Unfortunately, this technique is unsuitable for a distributed implementation. To circumvent this problem, we exploited the asymptotic expression at large K of the B-CB whose weights could be locally computed at every terminal and, further, well-approximate their original

counterparts. The performances of the so-obtained B-DCB technique were analyzed and compared to those of the M-DCB and B-CB techniques. We showed that the proposed B-DCB technique is able to reach its maximum achievable ASNR in lightly- to moderately-scattered environments while the achieved ASNR using the M-DCB technique, which is designed without taking into account the scattering effect, decreases in lightly-scattered environments and becomes soon unsatisfactory from moderately- to highly-scattered environments. We also showed that the proposed B-DCB technique achieves as much as 3 dB of ASNR gain in high scattering, when K is large enough. Moreover, we proved that for large K the achieved ASNR using the B-DCB technique approaches that achieved using the B-CB technique, which cannot be implemented in a distributed fashion.

APPENDIX A: PROOF OF THEOREM 1

It follows from (23) that

$$\tilde{P}_{\mathbf{w}_{\mathrm{BD}}}(\phi_\star)=\left(\frac{\mu_{\mathrm{D}}}{K}\right)^2(\mathrm{E}\{x_1\}+\mathrm{E}\{x_2\}+\mathrm{E}\{x_2^*\}+\mathrm{E}\{x_3\}),\ (45)$$

where

$$x_1=\mathbf{a}^H(\sigma_\theta)\mathbf{\Lambda}^{-1}\sum_{l=1}^L\alpha_l\mathbf{a}(\phi_\star+\theta_l)\sum_{m=1}^L\alpha_m^*\mathbf{a}^H(\phi_\star+\theta_m)\mathbf{\Lambda}^{-1}\mathbf{a}(\sigma_\theta)$$
$$(46)$$

$$x_2=\mathbf{a}^H(\sigma_\theta)\mathbf{\Lambda}^{-1}\sum_{l=1}^L\alpha_l\mathbf{a}(\phi_\star+\theta_l)\sum_{m=1}^L\alpha_m^*\mathbf{a}^H(\phi_\star+\theta_m)\mathbf{\Lambda}^{-1}\mathbf{a}(-\sigma_\theta)$$
$$(47)$$

$$x_3=\mathbf{a}^H(-\sigma_\theta)\mathbf{\Lambda}^{-1}\sum_{l=1}^L\alpha_l\mathbf{a}(\phi_\star+\theta_l)\sum_{m=1}^L\alpha_m^*\mathbf{a}^H(\phi_\star+\theta_m)\mathbf{\Lambda}^{-1}\mathbf{a}(-\sigma_\theta).$$
$$(48)$$

First, we derive the expression of x_1 as shown on the top of the next page. Using (9) in (49) yields

$$\mathrm{E}_{\alpha_l}\{x_1\}=\sum_{l=1}^L\frac{1}{L}\left(K+\sum_{k=1}^Ke^{j\frac{2\pi}{\lambda}r_k(\cos(\sigma_\theta-\psi_k)-\cos(\phi_\star+\theta_l-\psi_k))}\times\right.$$
$$\left.\sum_{s=1,s\neq k}^Ke^{-j\frac{2\pi}{\lambda}r_s(\cos(\sigma_\theta-\psi_s)-\cos(\phi_\star+\theta_l-\psi_s))}\right).\ (50)$$

However, we know that

$$\mathrm{E}_{r_k,\psi_k}\left\{e^{j\frac{2\pi}{\lambda}r_k(\cos(\sigma_\theta-\psi_k)-\cos(\phi_\star+\theta_l-\psi_k))}\right\}=2\frac{J_1(\gamma(\phi_\star+\theta_l-\sigma_\theta))}{\gamma(\phi_\star+\theta_l-\sigma_\theta)},$$
$$(51)$$

and, therefore,

$$\mathrm{E}\{x_1\}=K+4K(K-1)\int_\Theta p(\theta)\left(\frac{J_1(\gamma(\phi_\star+\theta-\sigma_\theta))}{\gamma(\phi_\star+\theta-\sigma_\theta)}\right)^2d\theta.\ (52)$$

Following similar steps as above, it can be shown that

$$\mathrm{E}\{x_2\}=2K\frac{J_1(\gamma(2\sigma_\theta))}{\gamma(2\sigma_\theta)}+4K(K-1)$$
$$\int_\Theta p(\theta)\frac{J_1(\gamma(\phi_\star+\theta-\sigma_\theta))}{\gamma(\phi_\star+\theta-\sigma_\theta)}\frac{J_1(\gamma(\phi_\star+\theta+\sigma_\theta))}{\gamma(\phi_\star+\theta+\sigma_\theta)}d\theta.\ (53)$$

As $\mathrm{E}\{x_2\}$ is real, $\mathrm{E}\{x_2\}=\mathrm{E}\{x_2^*\}$. In turn, x_3 is obtained by substituting σ_θ with $-\sigma_\theta$ in (49) and, hence,

$$\mathrm{E}\{x_3\}=K+4K(K-1)\int_\Theta p(\theta)\left(\frac{J_1(\gamma(\phi_\star+\theta+\sigma_\theta))}{\gamma(\phi_\star+\theta+\sigma_\theta)}\right)^2d\theta.\ (54)$$

Finally, using (52), (53) and (54) in (45), (28) is obtained.

On the other hand, from (5), the received noise power using $\mathbf{w}_{\mathrm{BD}}$ is given by

$$P_{\mathbf{w}_{\mathrm{BD}},n}=\left(\frac{\mu_{\mathrm{D}}}{K}\right)^2\left(\mathbf{a}^H(\sigma_\theta)+\mathbf{a}^H(-\sigma_\theta)\right)\mathbf{\Lambda}^{-1}\left(\mathbf{a}(\sigma_\theta)+\mathbf{a}(-\sigma_\theta)\right)+\sigma_n^2$$
$$=\left(\frac{\mu_{\mathrm{D}}}{K}\right)^2\left(2+\sum_{k=1}^Ke^{j\frac{2\pi}{\lambda}r_k(\cos(\psi_k+\sigma_\theta)-\cos(\psi_k-\sigma_\theta))}+\right.$$
$$\left.\sum_{k=1}^Ke^{-j\frac{2\pi}{\lambda}r_k(\cos(\psi_k+\sigma_\theta)-\cos(\psi_k-\sigma_\theta))}\right)+\sigma_n^2.\ (55)$$

Applying the expectation operator over both sides of (55) and using (21) in the resulting equation, (27) is obtained.

APPENDIX B: PROOF OF THEOREM 2

Using (24), the achieved beampattern by the M-DCB technique can be expressed as shown on the top of the next page. Thus, using (9) and the fact that

$$\mathrm{E}_{r_k,\psi_k}\left\{e^{j\frac{2\pi}{\lambda}r_k(\cos(\psi_k)-\cos(\phi_\star+\theta_l-\psi_k))}\right\}=2\frac{J_1(\gamma(\phi_\star+\theta_l))}{\gamma(\phi_\star+\theta_l)},$$
$$(57)$$

in (56), (33) is obtained.

In turn, from (5) the received noise power $P_{\mathbf{w}_{\mathrm{M}},n}$ is given by

$$P_{\mathbf{w}_{\mathrm{M}},n}=\frac{\sigma_v^2}{K^2}\mathbf{a}^H\mathbf{\Lambda}^{-1}\mathbf{a}+\sigma_n^2$$
$$=\frac{\sigma_v^2}{K}+\sigma_n^2.\ (58)$$

It follows from (58) that $\tilde{P}_{\mathbf{w}_{\mathrm{M}},n}=P_{\mathbf{w}_{\mathrm{M}},n}$ and, therefore, (32) is verified.

APPENDIX C: PROOF OF THEOREM 3

Using (17) we show that

$$\tilde{P}_{\mathbf{w}_{\mathrm{B}}}(\phi_\star)=\mathrm{E}\left\{\left(\frac{\mu}{K}\right)^2(x_1+x_2+x_2^*+x_3)\right\},\ (59)$$

and

$$\tilde{P}_{\mathbf{w}_{\mathrm{B}},n}=\mathrm{E}\left\{\left(\frac{\mu}{K}\right)^2\left(2+\sum_{k=1}^Ke^{j\frac{2\pi}{\lambda}r_k(\cos(\psi_k+\sigma_\theta)-\cos(\psi_k-\sigma_\theta))}+\right.\right.$$
$$\left.\left.\sum_{k=1}^Ke^{-j\frac{2\pi}{\lambda}r_k(\cos(\psi_k+\sigma_\theta)-\cos(\psi_k-\sigma_\theta))}\right)\right\}+\sigma_n^2.\ (60)$$

It is direct to show from (59) that

$$\lim_{K\to\infty}\tilde{P}_{\mathbf{w}_{\mathrm{B}}}(\phi_\star)=\mathrm{E}\left\{\left(\lim_{K\to\infty}\mu\right)^2\left(\lim_{K\to\infty}\frac{x_1}{K^2}+\lim_{K\to\infty}\frac{x_2}{K^2}+\right.\right.$$
$$\left.\left.\lim_{K\to\infty}\frac{x_2^*}{K^2}+\lim_{K\to\infty}\frac{x_3}{K^2}\right)\right\}.\ (61)$$

$$x_1 = \left(\mathbf{a}^H \left(\sigma_\theta \right) \mathbf{\Lambda}^{-1} \sum_{l=1}^{L} \alpha_l \mathbf{a}(\phi_\star + \theta_l) \right) \cdot \left(\sum_{m=1}^{L} \alpha_m^* \mathbf{a}^H (\phi_\star + \theta_m) \mathbf{\Lambda}^{-1} \mathbf{a} \left(\sigma_\theta \right) \right)$$

$$= \sum_{k=1}^{K} \sum_{s=1}^{K} \left(\sum_{l=1}^{L} |\alpha_l|^2 \, e^{j \frac{2\pi}{\lambda} r_k (\cos(\sigma_\theta - \psi_k) - \cos(\phi_\star + \theta_l - \psi_k))} \times e^{-j \frac{2\pi}{\lambda} r_s (\cos(\sigma_\theta - \psi_s) - \cos(\phi_\star + \theta_l - \psi_s))} + \right.$$

$$\left. \sum_{l=1}^{L} \alpha_l e^{j \frac{2\pi}{\lambda} r_k (\cos(\sigma_\theta - \psi_k) - \cos(\phi_\star + \theta_l - \psi_k))} \times \sum_{m=1, m \neq l}^{L} \alpha_m^* e^{-j \frac{2\pi}{\lambda} r_s (\cos(\sigma_\theta - \psi_s) - \cos(\phi_\star + \theta_m - \psi_s))} \right). \quad (49)$$

$$P_{\mathbf{w}_M} (\phi_\star) = \frac{1}{K^2} \left(\mathbf{a}^H \mathbf{\Lambda}^{-1} \sum_{l=1}^{L} \alpha_l \mathbf{a}(\phi_\star + \theta_l) \right) \cdot \left(\sum_{m=1}^{L} \alpha_m^* \mathbf{a}^H (\phi_\star + \theta_m) \mathbf{\Lambda}^{-1} \mathbf{a} \right)$$

$$= \frac{1}{K^2} \sum_{k=1}^{K} \sum_{s=1}^{K} \left(\sum_{l=1}^{L} |\alpha_l|^2 \, e^{j \frac{2\pi}{\lambda} r_k (\cos(\psi_k) - \cos(\phi_\star + \theta_l - \psi_k))} \times e^{-j \frac{2\pi}{\lambda} r_s (\cos(\psi_s) - \cos(\phi_\star + \theta_l - \psi_s))} + \right.$$

$$\left. \sum_{l=1}^{L} \alpha_l e^{j \frac{2\pi}{\lambda} r_k (\cos(\psi_k) - \cos(\phi_\star + \theta_l - \psi_k))} \times \sum_{m=1, m \neq l}^{L} \alpha_m^* e^{-j \frac{2\pi}{\lambda} r_s (\cos(\psi_s) - \cos(\phi_\star + \theta_m - \psi_s))} \right). \quad (56)$$

$$\lim_{K \to \infty} \frac{x_1}{K^2} = 4 \left(\sum_{l=1}^{L} |\alpha_l|^2 \left(\frac{J_1 \left(\gamma \left(\phi_\star + \theta_l - \sigma_\theta \right) \right)}{\gamma \left(\phi_\star + \theta_l - \sigma_\theta \right)} \right)^2 + \sum_{l=1}^{L} \alpha_l \frac{J_1 \left(\gamma \left(\phi_\star + \theta_l - \sigma_\theta \right) \right)}{\gamma \left(\phi_\star + \theta_l - \sigma_\theta \right)} \times \sum_{m=1, m \neq l}^{L} \alpha_m^* \frac{J_1 \left(\gamma \left(\phi_\star + \theta_m - \sigma_\theta \right) \right)}{\gamma \left(\phi_\star + \theta_m - \sigma_\theta \right)} \right). \quad (62)$$

$$\lim_{K \to \infty} \frac{x_2}{K^2} = 4 \left(\sum_{l=1}^{L} |\alpha_l|^2 \frac{J_1 \left(\gamma (\phi_\star + \theta_l - \sigma_\theta) \right)}{\gamma (\phi_\star + \theta_l - \sigma_\theta)} \times \frac{J_1 \left(\gamma \left(\phi_\star + \theta_l + \sigma_\theta \right) \right)}{\gamma \left(\phi_\star + \theta_l + \sigma_\theta \right)} + \sum_{l=1}^{L} \alpha_l \frac{J_1 \left(\gamma (\phi_\star + \theta_l - \sigma_\theta) \right)}{\gamma (\phi_\star + \theta_l - \sigma_\theta)} \times \sum_{m=1, m \neq l}^{L} \alpha_m^* \frac{J_1 \left(\gamma (\phi_\star + \theta_m + \sigma_\theta) \right)}{\gamma (\phi_\star + \theta_m + \sigma_\theta)} \right) \quad (63)$$

$$\lim_{K \to \infty} \frac{x_3}{K^2} = 4 \left(\sum_{l=1}^{L} |\alpha_l|^2 \left(\frac{J_1 \left(\gamma \left(\phi_\star + \theta_l + \sigma_\theta \right) \right)}{\gamma \left(\phi_\star + \theta_l + \sigma_\theta \right)} \right)^2 + \sum_{l=1}^{L} \alpha_l \frac{J_1 \left(\gamma \left(\phi_\star + \theta_l + \sigma_\theta \right) \right)}{\gamma \left(\phi_\star + \theta_l + \sigma_\theta \right)} \times \sum_{m=1, m \neq l}^{L} \alpha_m^* \frac{J_1 \left(\gamma \left(\phi_\star + \theta_m + \sigma_\theta \right) \right)}{\gamma \left(\phi_\star + \theta_m + \sigma_\theta \right)} \right). \quad (64)$$

Using the strong law of large numbers and (51), we can obtain (62), (63) and (64). Moreover, we can easily prove that $\lim_{K \to \infty} x_2^* / K^2 = \lim_{K \to \infty} x_2 / K^2$. Substituting (62), (63) and (64) in (61) and using (22) and the property in (9) yields

$$\lim_{K \to \infty} \tilde{P}_{\mathbf{w}_B} (\phi_\star) = \lim_{K \to \infty} \tilde{P}_{\mathbf{w}_{BD}} (\phi_\star). \quad (65)$$

Furthermore, we can show that

$$\lim_{K \to \infty} \tilde{P}_{\mathbf{w}_B, n} = \lim_{K \to \infty} \tilde{P}_{\mathbf{w}_{BD}, n}. \quad (66)$$

(43) can then be inferred from (65) and (66).

APPENDIX D: PROOF OF THEOREM 4

To prove (44), we first focus on the achieved ASNR $\bar{\xi}_{\mathbf{w}_{BD}}$ given by

$$\bar{\xi}_{\mathbf{w}_{BD}} = E \left\{ \frac{P_{\mathbf{w}_{BD}}(\phi_s)}{P_{\mathbf{w}_{BD}, n}} \right\}. \quad (67)$$

From (67), we have

$$\lim_{K \to \infty} \bar{\xi}_{\mathbf{w}_{BD}} = E \left\{ \frac{\lim_{K \to \infty} P_{\mathbf{w}_{BD}}(\phi_s)}{\lim_{K \to \infty} P_{\mathbf{w}_{BD}, n}} \right\}. \quad (68)$$

It is direct to show from (55) that

$$\lim_{K \to \infty} P_{\mathbf{w}_{BD}, n} = \sigma_n^2, \quad (69)$$

and, hence,

$$\lim_{K \to \infty} \bar{\xi}_{\mathbf{w}_{BD}} = \frac{E \left\{ \lim_{K \to \infty} P_{\mathbf{w}_{BD}}(\phi_s) \right\}}{\sigma_n^2}. \quad (70)$$

Moreover, we have

$$E \left\{ \lim_{K \to \infty} P_{\mathbf{w}_{BD}} (\phi_\star) \right\} = \mu_D^2 E \left\{ \left(\lim_{K \to \infty} \frac{x_1}{K^2} + 2 \lim_{K \to \infty} \frac{x_2}{K^2} + \right. \right.$$

$$\left. \left. \lim_{K \to \infty} \frac{x_3}{K^2} \right) \right\}. \quad (71)$$

Substituting (62), (63) and (64) in (71), we show that $E \{ \lim_{K \to \infty} P_{\mathbf{w}_{BD}} (\phi_\star) \} = \lim_{K \to \infty} \tilde{P}_{\mathbf{w}_{BD}} (\phi_\star)$. Using this result in (70), (44) is obtained for $\mathbf{w} = \mathbf{w}_{BD}$.

Using the same method as above, (44) can be also proved for $\mathbf{w} = \mathbf{w}_M$ and $\mathbf{w} = \mathbf{w}_B$.

REFERENCES

[1] H. Ochiai, P. Mitran, H. V. Poor, and V. Tarokh, "Collaborative beamforming for distributed wireless ad hoc sensor networks," *IEEE Trans. Signal Process.*, vol. 53, pp. 4110–4124, Nov. 2005.
[2] M. F. A. Ahmed and S. A. Vorobyov, "Collaborative beamforming for wireless sensor networks with Gaussian distributed sensor nodes," *IEEE Trans. Wireless Commun.*, vol. 8, pp. 638–643, Feb. 2009.

[3] J. Huang, P. Wang, and Q. Wan, "Collaborative beamforming for wireless sensor networks with arbitrary distributed sensors," *IEEE Commun. Lett.,* vol. 16, pp. 1118–1120, July 2012.

[4] K. Zarifi, A. Ghrayeb, and S. Affes , "Distributed beamforming for wireless sensor networks with improved graph connectivity and energy efficiency," *IEEE Trans. Signal Process.,* vol. 58, pp. 1904–1921, Mar. 2010.

[5] M. F. A. Ahmed and S. A. Vorobyov, "Sidelobe control in collaborative beamforming via node selection," *IEEE Trans. Signal Process.,* vol. 58, pp. 6168–6180, Dec. 2010.

[6] R. Mudumbai, G. Barriac, and U. Madhow, "On the feasibility of distributed beamforming in wireless networks," *IEEE Trans. Wireless Commun.,* vol. 6, pp. 1754–1763, May 2007.

[7] R. Mudumbai, D. R. Brown, U. Madhow, and H. V. Poor, "Distributed transmit beamforming: challenges and recent progress," *IEEE Commun. Mag.,* vol. 47, pp. 102–110, Feb. 2009.

[8] Z. Han and H. V. Poor, "Lifetime improvement in wireless sensor networks via collaborative beamforming and cooperative transmission," *IET Microw. Antennas Propag.,* vol. 1, pp. 1103–1110, Dec. 2007.

[9] L. Dong, A. P. Petropulu, and H. V. Poor, "A cross-layer approach to collaborative beamforming for wireless ad hoc networks," *IEEE Trans. Signal Process.,* vol. 56, pp. 2981–2993, July 2008.

[10] L. C. Godara, "Application of antenna arrays to mobile communications—part II: beam-forming and direction-of-arrival considerations," *Proc. IEEE,* vol. 85, pp. 1195–1245, Aug. 1997.

[11] K. Zarifi, S. Zaidi, S. Affes, and A. Ghrayeb, "A distributed amplify-and-forward beamforming technique in wireless sensor networks," *IEEE Trans. Signal Process.,* vol. 59, pp. 3657–3674, Aug. 2011.

[12] K. Zarifi, S. Affes, and A. Ghrayeb, "Collaborative null-steering beamforming for uniformly distributed wireless sensor networks," *IEEE Trans. Signal Process.,* vol. 58, pp. 1889–1903, Mar. 2010.

[13] D. Astly and B. Ottersten, "The effects of local scattering on direction of arrival estimation with MUSIC," *IEEE Trans. Signal Process.,* vol. 47, pp. 3220–3234, Dec. 1999.

[14] A. Amar, "The effect of local scattering on the gain and beamwidth of a collaborative beampattern for wireless sensor networks," *IEEE Trans. Wireless Commun.,* vol. 9, pp. 2730–2736, Sept. 2010.

[15] O. Besson, P. Stoica, and A. B. Gershman, "Simple and accurate direction of arrival estimator in the case of imperfect spatial coherence," *IEEE Trans. Signal Process.,* vol. 49, pp. 730-737, Apr. 2001.

[16] S. Shahbazpanahi, S. Valaee, and A. B. Gershman, "A covariance fitting approach to parametric localization of multiple incoherently distributed sources," *IEEE Trans. Signal Process.,* vol. 52, pp. 592–600, Mar. 2004.

[17] M. Souden, S. Affes, and J. Benesty, "A two-stage approach to estimate the angles of arrival and the angular spreads of locally scattered sources," *IEEE Trans. Signal Process.,* vol. 56, pp. 1968–1983, May 2008.

[18] M. Bengtsson and B. Ottersten, "Low-complexity estimators for distributed sources," *IEEE Trans. Signal Process.,* vol. 48, pp. 2185–2194, Aug. 2000.

[19] V. Havary-Nassab, S. Shahbazpanahi, A. Grami, and Z.-Q. Luo, "Distributed beamforming for relay networks based on second-order statistics of the channel state information," *IEEE Trans. Signal Process.,* vol. 56, pp. 4306–4316, Sept. 2008.

[20] I. Thibault, A. Faridi, G. E. Corazza, A. V. Coralli, and A. Lozano, "Design and analysis of deterministic distributed beamforming algorithms in the presence of noise," *IEEE Trans. Commun.,* vol. 61, pp. 1595–1607, Apr. 2013.

[21] R. Mudumbai, J. Hespanha, U. Madhow, and G. Barriac, "Distributed transmit beamforming using feedback control," *IEEE Trans. Inf. Theory,* vol. 56, pp. 411–426, Jan. 2010.

[22] D. R. Brown and H. V. Poor, "Time-slotted round trip carrier synchronization for distributed beamforming," *IEEE Trans. Signal Process.,* vol. 56, pp. 5630–5643, Nov. 2008.

[23] B. D. Van Veen and K. M. Buckley, "Beamforming: a versatile approach to spatial filtering," *IEEE ASSP Mag.,* vol. 5, pp. 4-24, Apr. 1988.

[24] S. Affes, S. Gazor, and Y. Grenier, "An algorithm for multisource beamforming and multitarget tracking," *IEEE Trans. Signal Process.,* vol. 44, pp. 1512–1522, June 1996.

[25] S. Zaidi and S. Affes, "Distributed beamforming for wireless sensor networks in local scattering environments," in *Proc. 2012 IEEE VTC – Fall.*

[26] S. Zaidi and S. Affes, "Distributed collaborative beamforming with minimum overhead for local scattering environments," *Proc. 2012 IEEE IWCMC,* invited paper.

[27] D. Cox, "Cochannel interference considerations in frequency reuse small-coverage-area radio systems," *IEEE Trans. Commun.,* vol. 30, pp. 135–142, Jan. 1982.

[28] A. Anderson, J. Zeidler, and M. Jensen, "Reduced-feedback linear precoding with stable performance for the time-varying MIMO broadcast channel," *IEEE J. Sel. Areas Commun.,* vol. 26, pp. 1483–1493, Oct. 2008.

[29] I. S. Gradshteyn and I. M. Ryzhik, *Table of Integrals, Series and Products,* 5th ed. Academic, 1994.

[30] S. Zaidi and S. Affes, "SNR and throughput analysis of distributed collaborative beamforming in locally-scattered environments," *Wiley J. Wireless Commun. Mobile Comput.,* vol. 12, pp. 1620–1633, Dec. 2012, invited paper.

[31] S. Zaidi and S. Affes, "Analysis of collaborative beamforming designs in real-world environments," in *Proc. 2013 IEEE WCNC.*

[32] S. Zaidi and S. Affes, "Spectrum-efficient distributed collaborative beamforming in the presence of local scattering and interference," in *Proc. 2012 IEEE GLOBECOM.*

Slim Zaidi received the B.Eng. degree in Telecommunications from the National Engineering School of Tunis, Tunisia, in 2008 and the M.Sc. degree from INRS-EMT, Université du Québec, Montreal, Quebec, Canada in 2011, both with highest honors. He is currently pursuing the Ph.D. degree at INRS-EMT. His research interests include statistical signal and array processing, MIMO, cooperative communications, and wireless sensor networks. Mr. Zaidi received the National Grant of Excellence from the Tunisian Government for both the M.Sc. (2009-2010) and the PhD. (2011-2013) programs and is currently recipient of a top-tier graduate scholarship from the National Sciences and Engineering Research Council (2013-2015). He had to decline another prestigious Ph.D. scholarship offered over the same period from the "Fonds de Recherche du Québec Nature et Technologies" (FRQNT). He acts regularly as a reviewer for many international scientific journals and conferences.

Sofiène Affes (IEEE SM04) received the Diplôme d'Ingénieur in telecommunications in 1992, and the Ph.D. degree with honors in signal processing in 1995, both from École Nationale Supérieure des Télécommunications (ENST), Paris, France. He has been since with INRS, Canada, as a Research Associate till 1997, an Assistant Professor till 2000, and Associate Professor till 2009. Currently he is Full Professor and Director of PERWADE, a unique 4M$ research training program on wireless in Canada involving 27 faculty from eight universities and 10 industrial partners. Dr Affes has been twice the recipient of a Discovery Accelerator Supplement Award from NSERC, from 2008 to 2011, and from 2013 to 2016. From 2003 to 2013, he held a Canada Research Chair in Wireless Communications. In 2006, he served as a General Co-Chair of IEEE VTC2006-Fall, Montreal, Canada. In 2008 he received from the IEEE Vehicular Technology Society the IEEE VTC Chair Recognition Award for exemplary contributions to the success of IEEE VTC. He currently acts as an Associate Editor for the IEEE TRANSACTIONS ON COMMUNICATIONS, the IEEE TRANSACTIONS ON SIGNAL PROCESSING, and the *Wiley Journal on Wireless Communications & Mobile Computing*. From 2007 till 2013, he has been an Associate Editor for the IEEE TRANSACTIONS ON WIRELESS COMMUNICATIONS. He is serving now as a General Co-Chair of IEEE ICUWB to be held in Montreal in the fall 2015.